Proceedings of the 10th International Conference on Civil Structural and Transportation Engineering (ICCSTE 2025)
July, 2025 | Imperial College London Conference Center, London, United Kingdom
Paper No. 138
DOI: 10.11159/iccste25.138

Comparative Assessment of CFQST vs Traditional Columns under Lateral Loads

Ishan Jha[1*], Sekhar Chandra Dutta[2], Ganga Kasi Viswanadh Prakhya[3], Vikash Kumar[4]
[1]Postdoctoral fellow, Department of Civil Engineering, Indian Institute of Technology (ISM), Dhanbad, Jharkhand, India E-mail: ishanjha93@gmail.com, 23pf0162@iitism.ac.in (Presenting author)
[2]Professor, Department of Civil Engineering, Indian Institute of Technology (ISM), Dhanbad, Jharkhand, India E-mail: scdind2000@gmail.com, sekhar@iitism.ac.in
[3]Director, Design Group, Sir Robert McAlpine, Hemel Hempstead, United Kingdom, E-mail: kvgprakhya@gmail.com
[4]Research Scholar, Department of Civil Engineering, Indian Institute of Technology (ISM), Dhanbad, Jharkhand, India E-mail: vikashkr23dr@gmail.com, 23dr0200@iitism.ac.in

Abstract - The study presents a comparative computational analysis of proposed Concrete-Filled Quadruple Steel Tubular (CFQST) columns, concentrating on their lateral load-bearing capacity, lateral ductility, and concrete durability which are essential factors for evaluating seismic risk management. Validated finite element simulations with varying concrete strengths (M25, M40, M50) and slenderness ratios (7, 14, 20) reveal that CFQST columns outperform Reinforced Concrete (RCC), Concrete-Filled Steel Tubular (CFST), and Concrete-Filled Double Steel Tubular (CFDST) columns. CFQST columns demonstrate up to 2.37 times greater lateral load capacity and 1.75 times higher ductility than RCC. When compared to CFST and CFDST columns, CFQST columns offer 1.11 to 1.68 times greater ductility and 1.16 to 1.54 times higher lateral load capacity. The improved performance is due to the confinement effects of four internal steel tubes encased in concrete and confined by an outer steel tube, enhancing the durability of the encased concrete and delaying crushing, resulting in higher energy absorption. The observed "elephant foot" ductile buckling confirms the columns' effectiveness in mitigating the brittle behaviour of concrete. These findings establish CFQST columns as a resilient, durable, and sustainable solution, particularly well-suited for seismic regions and high-risk environments, with significant potential for reducing long-term life cycle costs.

Keywords**:** CFQST columns, Lateral ductility, Concrete durability, Seismic performance, Confinement effect, Structural resilience

1. Introduction

The lateral performance and durability of structural columns are crucial for designing resilient infrastructure, especially in seismic and high-risk areas [1]. Columns endure complex axial, lateral, and torsional loads, requiring a thorough understanding of their behaviour to ensure stability and durability [2]. While RCC columns are widely used, their brittle nature and susceptibility to cracking under lateral loads pose challenges, particularly in seismic zones where high energy dissipation, ductility, and robustness are essential [3,4].

Composite columns, such as Concrete-Filled Steel Tubular (CFST) columns, are gaining popularity for overcoming RCC limitations [5]. CFST columns combine concrete's compressive strength with the tensile and confining benefits of a steel tube, enhancing lateral performance and deformation capacity [6]. However, under severe loading, such as high slenderness ratios or variable lateral loads, CFST columns may experience localized failures or buckling due to insufficient confinement [7]. Concrete-Filled Double Steel Tubular (CFDST) columns, featuring an additional inner steel tube, address these issues by providing dual confinement, enhancing lateral resistance, delaying crack initiation, and improving ductility [8]. Yet, CFDST columns face challenges in optimizing stress distribution and ensuring durability, especially in slender or high-strength configurations [9].

Addressing these challenges, the innovative Concrete-Filled Quadruple Steel Tubular (CFQST) column offers a transformative approach. This configuration presented in this study incorporates four internal steel tubes symmetrically embedded within the concrete core, confined by an outer steel tube. This unique design provides multiple layers of confinement, mitigating stress concentrations, enhancing lateral load-carrying capacity, and significantly improving ductility. The strategic placement of internal steel tubes ensures uniform stress distribution, delays local buckling, and prevents brittle failure, while the outer steel tube contributes to overall structural stability and energy absorption. Finite

Element Method (FEM) methodologies have long been employed to solve a wide range of structural engineering problems [10,11], enabling researchers to reduce experimental costs while obtaining highly reliable and detailed results. Leveraging these advantages, this study presents a comparative computational analysis of CFQST columns against traditional RCC, CFST, and CFDST columns, focusing on lateral performance and concrete durability. Using validated finite element models, the analysis examines the influence of varying concrete strengths (M25, M40, M50) and slenderness ratios on the columns' behaviour under lateral loading. Key performance metrics, such as lateral load-bearing capacity, ductility, and failure modes, are evaluated to establish the advantages of CFQST columns. A previous experimental study demonstrated the superior axial load-carrying capacity and axial ductility of CFQST columns compared to other column types. The CFQST columns exhibited a 42% increase in axial load capacity and a remarkable 103% improvement in axial ductility over RCC columns. However, the lateral load-carrying capacity and ductility of these columns remained unexplored. In this context, the present study employs a computational model, validated against the prior experimental results, to investigate the lateral load-carrying capacity and ductility of the same column types. Additional sets of columns are analysed to further evaluate whether CFQST columns consistently exhibit superior performance under lateral loading, as observed in the axial capacity tests.

2. Methodology

This study employs a computational approach to analyse the lateral performance and durability of CFQST columns compared to RCC, CFST, and CFDST columns. Finite element analysis was conducted using ABAQUS, chosen for its ability to simulate nonlinear material behaviour and complex structural interactions under lateral loads. Uniform cross-sectional dimensions of 150 mm × 150 mm were used across all column types for consistent comparison. The CFQST columns, featuring four internal steel tubes within a concrete core and an outer steel tube, were modelled alongside RCC, CFST (single steel tube), and CFDST (dual steel tubes) columns. Geometric configurations were precisely replicated, with Fig. 1 illustrating schematics for each type. The analysis emphasized steel-concrete interaction, highlighting the enhanced confinement offered by CFQST columns.

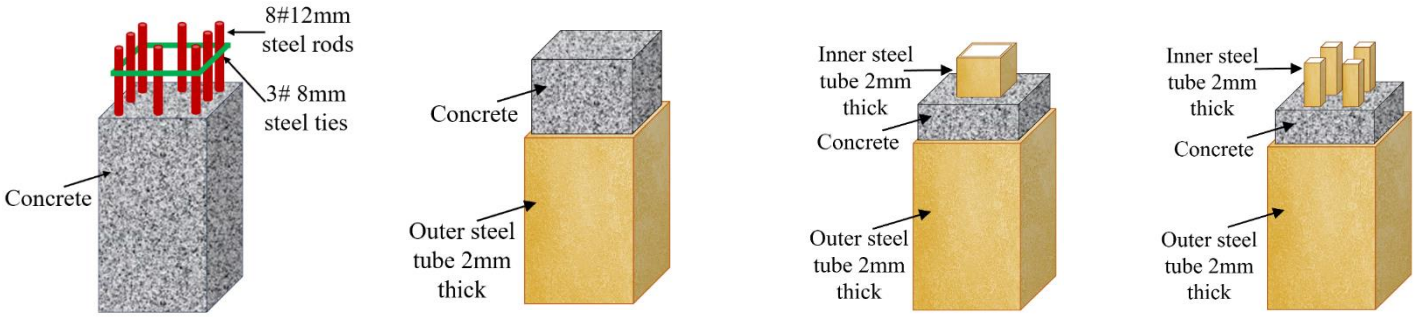

(a) RCC column (b) CFST column (c) CFDST column (d) CFQST column

Fig. 1: Different types of columns.

Material modelling played a pivotal role in capturing the structural behaviour of the columns. Concrete was simulated using the Concrete Damage Plasticity (CDP) model, which effectively characterizes the nonlinear stress-strain relationship, damage parameters, and failure mechanisms under multiaxial loading. Four grades of concrete (M25, M40, and M50) were incorporated to study the influence of varying compressive strengths. The stress-strain curve for confined concrete was modelled in three stages – elastic, strain hardening, and strain softening – following the formulations proposed by Tao et al. [12]. The elastic modulus of confined concrete was computed using ACI recommendations, and a Poisson's ratio of 0.18 was adopted. The parameters for the CDP model were carefully calibrated, including the dilation angle, flow potential eccentricity, and the biaxial-to-uniaxial compressive strength ratio, ensuring accurate simulation of the concrete's nonlinear behaviour.

Steel tubes, both internal and external, were modelled as elastic-plastic materials with properties derived from experimental coupon tests. These tests provided the yield strength (251.3 N/mm²), ultimate strength (328 N/mm²), and elastic elastic modulus (2.01×10^5 N/mm²) used in the numerical simulations. The interaction between steel and concrete components components was defined using surface-to-surface cohesive contact, incorporating a friction coefficient of 0.6 to simulate realistic bonding and sliding behaviour. Boundary and loading conditions were designed to replicate experimental setups with high fidelity for validation purpose. Fixed supports were applied at the base to restrict all degrees of freedom, while a lateral displacement-controlled load was applied incrementally at the top of the column. A kinematic coupling mechanism was employed to ensure uniform transfer of displacement and rotation among the steel and concrete components. This configuration effectively captured the response of the columns under combined axial and lateral loading conditions. FEM models of the four columns is shown in Fig. 2

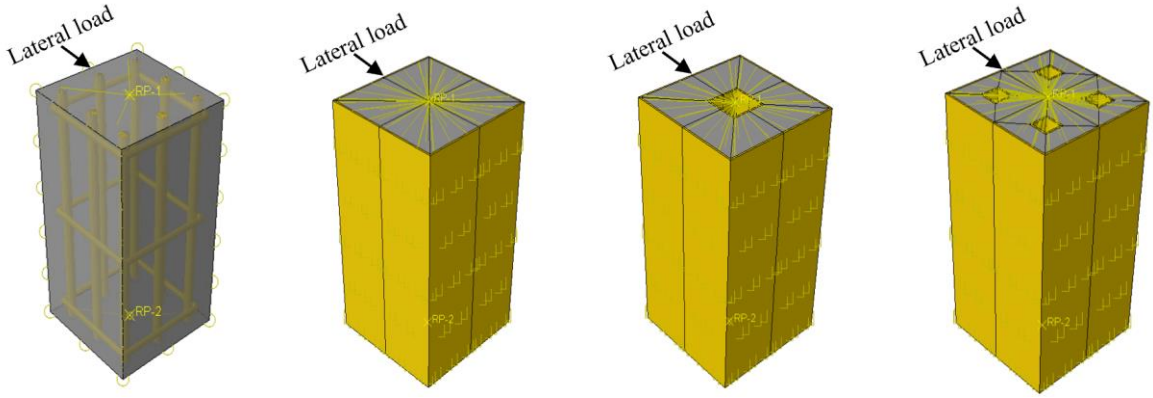

(a) RCC (b) CFST (c) CFDST (d) CFQST

Fig. 2 Laterally loaded columns.

3. Validation of finite element models

Validation of the finite element models was conducted using experimental results obtained from controlled laboratory tests. Axial loading experiments were performed on specimens with a square cross-section of 150 mm and a height of 305 mm. The tests were carried out using a compression testing machine with a 3000 kN capacity, equipped with LVDTs and strain gauges to measure deformations with high precision. The finite element models were designed to replicate the experimental setup, including the kinematic coupling mechanism and displacement-controlled loading conditions. Table 1 summarizes the results obtained from both experimental testing and finite element analysis, while Fig. 3 illustrates the corresponding load-displacement graphs.

Table 1: Comparison in experimental and FEM results for axial load-carrying capacities and ductility of RCC, CFST, CFDST, and CFQST columns.

Column	Hollow ratio (χ)	Concrete	Length (mm)	Experimental		Finite element model	
				A_u (kN)	Axial D_y	A_u (kN)	Axial D_y
C-1 (*RCC*)	–	25	305	1015.99	1.39	1083.21	1.35
C-2 (*CFST*)	–	25	305	1396.05	2.05	1398.72	1.94
C-3 (*CFDST*)	0.27	25	305	1377.22	2.63	1389.73	2.59
C-4 (*CFQST*)	0.27	25	305	1449.97	2.82	1475.52	2.84

where, A_u = Axial load-carrying capacity of the columns, D_y = Ductility as per the deformation at yield load.

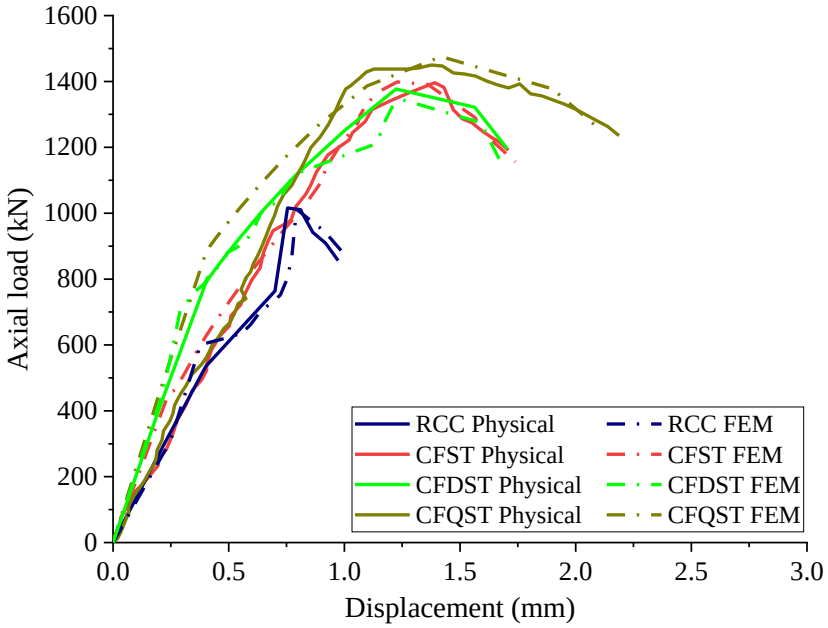

Fig. 3: Load-displacement curves obtained using experimental and FEM analysis.

A comparison of experimental and numerical results showed a mean absolute percentage error (MAPE) of 2.36% for axial load capacity and 2.61% for axial ductility, confirming the accuracy of the numerical models. These validated models were then used for extensive simulations to evaluate the lateral load capacity, ductility, and durability of CFQST columns compared to RCC, CFST, and CFDST columns. The simulations provided detailed insights into the superior performance of CFQST columns under seismic and high-stress conditions.

4. Results and discussion

This study evaluates the lateral performance and durability of CFQST columns compared to RCC, CFST, and CFDST columns. A total of 36 columns, grouped into nine sets, were analysed, with each set including one RCC, one CFST, one CFDST, and one CFQST column. The sets systematically varied concrete strength and column slenderness to examine material and geometric effects on lateral performance. Key metrics, including lateral load capacity, ductility, and energy dissipation, were assessed. RCC columns served as references for comparing lateral performance. The results emphasize the influence of advanced confinement mechanisms, material properties, and geometry on column behaviour under lateral loads, with ductility evaluated using a well-established approach from the literature. This methodology utilizes pre-peak and post-peak displacement parameters from the load-displacement curve to quantitatively assess each column's deformation capacity. Lateral ductility (D_y) is calculated using the relationship in Eq. 1.

$$D_y = \frac{\delta_{0.85}}{\delta_y} \tag{3}$$

where δ_y denotes the displacement at the yield load. The yield load is conventionally defined as 75% of the ultimate load on the ascending portion of the load-displacement curve. $\delta_{0.85}$ considers the displacement at 85% of the ultimate load on the descending portion of the curve.

Table 2 summarizes the FEM-based results, offering detailed comparisons across column types and configurations. The load-displacement behaviour, shown in Fig. 4, highlights the superior lateral resistance and ductility of CFQST columns, aligning with the findings in Table 2. These results provide valuable insights into the structural advantages of

CFQST columns and the factors influencing their performance. The subsequent sections detail the observed trends and performance enhancements with technical precision.

Table 2: Comparative analysis of lateral load-carrying capacities and ductility for RCC, CFST, CFDST, and CFQST columns.

Set No.	Column	Hollow ratio (χ)	Concrete	Length	L_u (kN)	Lateral D_y	$\frac{L_u}{L_{uRCC}}$	$\frac{Lateral\ D_y}{Lateral\ D_{yRCC}}$
Set-1	C-1 (*RCC*)	–	25	305	48.77	7.03	1	1
	C-2 (*CFST*)	–	25	305	75.47	7.82	1.54	1.11
	C-3 (*CFDST*)	0.27	25	305	99.79	11.19	2.04	1.59
	C-4 (*CFQST*)	0.27	25	305	115.81	12.71	2.37	1.81
Set-2	C-5 (*RCC*)	–	40	305	58.07	5.51	1	1
	C-6 (*CFST*)	–	40	305	91.99	5.81	1.58	1.05
	C-7 (*CFDST*)	0.27	40	305	122.19	7.85	2.10	1.42
	C-8 (*CFQST*)	0.27	40	305	143.59	9.28	2.47	1.68
Set-3	C-9 (*RCC*)	–	50	305	64.11	5.19	1	1
	C-10 (*CFST*)	–	50	305	98.54	5.67	1.54	1.09
	C-11 (*CFDST*)	0.27	50	305	133.07	7.54	2.08	1.45
	C-12 (*CFQST*)	0.27	50	305	156.33	8.78	2.44	1.69
Set-4	C-13 (*RCC*)	–	25	600	25.05	4.27	1	1
	C-14 (*CFST*)	–	25	600	35.84	4.59	1.43	1.07
	C-15 (*CFDST*)	0.27	25	600	47.64	7.01	1.90	1.64
	C-16 (*CFQST*)	0.27	25	600	56.24	7.62	2.25	1.78
Set-5	C-17 (*RCC*)	–	40	600	30.94	3.32	1	1
	C-18 (*CFST*)	–	40	600	41.34	3.57	1.34	1.08
	C-19 (*CFDST*)	0.27	40	600	56.33	5.18	1.82	1.56
	C-20 (*CFQST*)	0.27	40	600	69.06	5.79	2.23	1.74
Set-6	C-21 (*RCC*)	–	50	600	33.37	3.59	1	1
	C-22 (*CFST*)	–	50	600	45.97	3.74	1.38	1.04
	C-23 (*CFDST*)	0.27	50	600	57.89	4.47	1.73	1.25
	C-24 (*CFQST*)	0.27	50	600	74.56	5.57	2.23	1.55
Set-7	C-25 (*RCC*)	–	25	900	17.96	3.83	1	1
	C-26 (*CFST*)	–	25	900	27.31	4.38	1.52	1.14
	C-27 (*CFDST*)	0.27	25	900	36.32	5.71	2.02	1.49
	C-28 (*CFQST*)	0.27	25	900	41.12	6.65	2.29	1.74
Set-8	C-29 (*RCC*)	–	40	900	20.88	3.14	1	1
	C-30 (*CFST*)	–	40	900	32.48	3.51	1.56	1.12
	C-31 (*CFDST*)	0.27	40	900	42.69	4.31	2.04	1.37
	C-32 (*CFQST*)	0.27	40	900	48.96	5.27	2.34	1.68
Set-9	C-33 (*RCC*)	–	50	900	23.42	2.67	1	1
	C-34 (*CFST*)	–	50	900	35.33	3.05	1.51	1.14
	C-35 (*CFDST*)	0.27	50	900	46.57	3.68	1.99	1.38

	C-36 (*CFQST*)	0.27	50	900	53.91	4.78	2.30	1.79
Note: The RCC column of each set is designated as the reference for comparative evaluation of lateral load-carrying capacity and ductility in that set.								

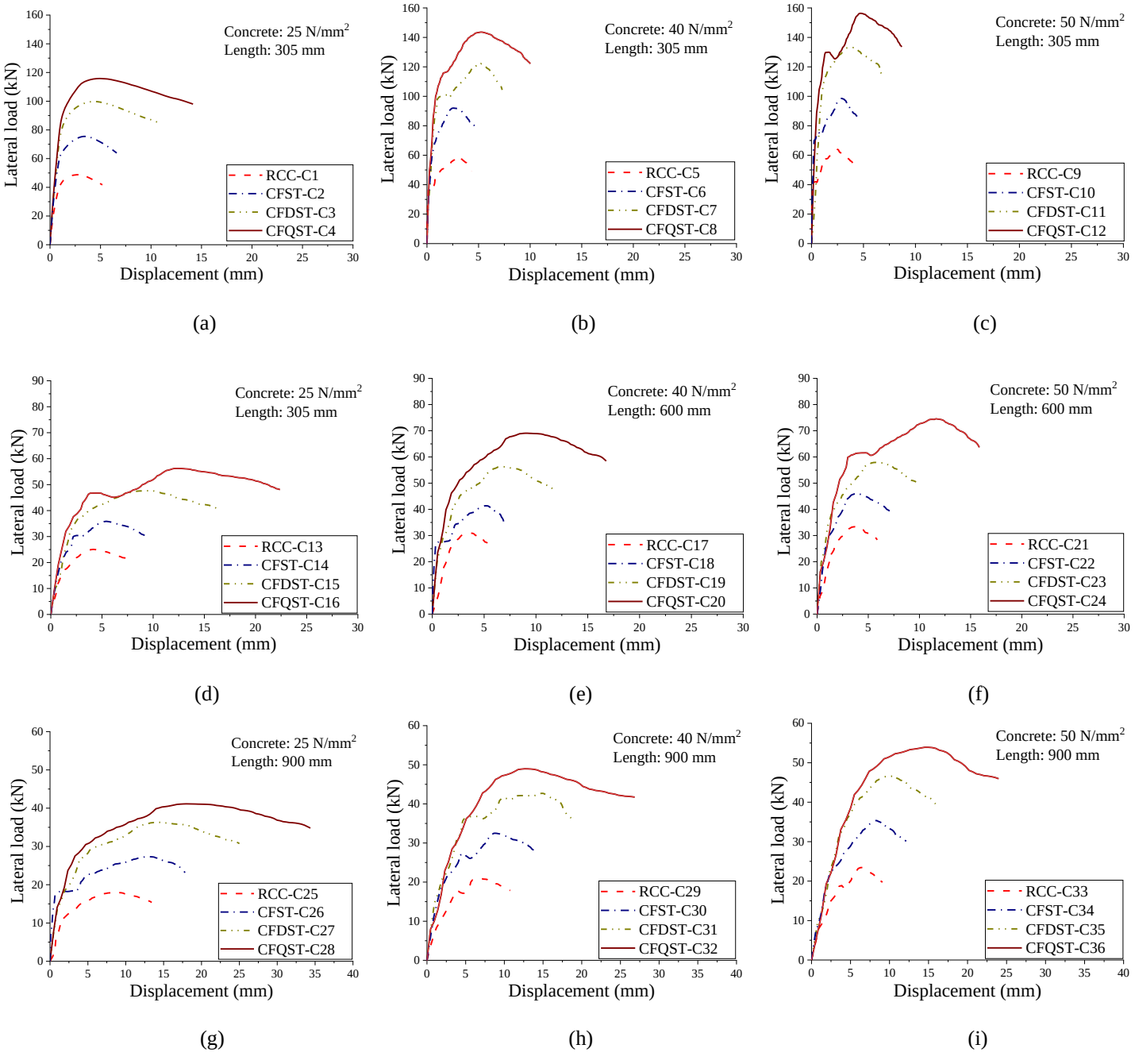

Fig. 4: Load-displacement curves obtained for different types of columns.

4.1. Lateral Load-Carrying Capacity

The lateral load-carrying capacity is significantly affected by structural configuration, material properties, and slenderness ratio. CFQST columns consistently outperformed other types, with an average ultimate lateral load capacity 133% higher than RCC, 57% higher than CFST, and 20% higher than CFDST columns. For short columns (305 mm length), length), CFQST columns demonstrated exceptional load-carrying capacities. At 25 MPa concrete strength, the CFQST column (C-4) achieved an ultimate load of 115.81 kN, outperforming RCC (C-1) by 2.37 times, CFST (C-2) by 1.54 times, and CFDST (C-3) by 1.16 times. This performance is attributed to enhanced confinement from quadruple internal and external steel tubes, improving stress distribution and delaying failure. At 40 MPa and 50 MPa, CFQST columns-maintained dominance with ultimate loads of 143.59 kN and 156.33 kN, 2.47 and 2.44 times the capacity of RCC columns (C-5 and C-9). CFDST columns showed intermediate performance, achieving ~110% higher load capacity than RCC columns. For medium-length columns (600 mm), increased slenderness reduced load-carrying capacities across all types, but CFQST columns remained superior. At 25 MPa, the CFQST column (C-16) achieved a load of 56.24 kN, 2.25 times that of RCC (C-13), thanks to its confinement mechanism mitigating buckling effects. In long columns (900 mm), the performance gap widened. At 25 MPa, CFQST (C-28) reached 41.12 kN, 2.29 times RCC (C-25). At higher strengths, CFQST columns consistently outperformed CFDST and CFST by 17% and 51%, respectively, on average.

4.2. Lateral Ductility

Lateral ductility, crucial for seismic resilience, was evaluated using pre- and post-peak displacements from load-displacement curves. On average, CFQST columns demonstrated 75% greater ductility than RCC columns, 47% more than CFST columns, and 16% more than CFDST columns. For short columns (305 mm), CFQST columns showed superior ductility ratios. At 25 MPa, the ductility of the CFQST column (C-4) was 12.71, 1.81 times that of the RCC column (C-1), due to enhanced energy dissipation from internal and external steel tubes. In medium-length columns (600 mm), CFQST columns maintained their advantage, with C-16 achieving a ductility of 7.62 – 1.78 times higher than RCC (C-13) and 1.08 times higher than CFDST (C-15). For long columns (900 mm), ductility decreased across all types due to slenderness, but CFQST columns still excelled. At 25 MPa, C-28 had a ductility of 6.65, 1.74 times higher than RCC (C-25) and 1.16 times higher than CFDST (C-27), proving their effectiveness in resisting lateral deformations even under slender conditions.

Fig. 4 shows that higher concrete strength increases lateral load capacity across all column types due to improved compressive strength but reduces ductility due to the brittle nature of high-strength concrete. Longer columns exhibit higher displacement capacities but reduced peak strength due to slenderness and buckling, with RCC columns most affected. CFST, CFDST, and CFQST columns perform better due to effective composite action and enhanced confinement. The predominant failure mode observed is "elephant foot" buckling, with CFST, CFDST, and CFQST columns demonstrating greater resistance to this mode, showcasing superior structural behaviour compared to RCC columns under varying strengths and lengths.

5. Conclusion

Present study comprehensively evaluated the lateral performance of CFQST columns in comparison to RCC, CFST, and CFDST columns under varying conditions of concrete strength, slenderness ratio, and hollow ratios. A total of 36 columns were evaluated through finite element modelling. The models were validated against experimental results as mentioned earlier. The findings highlight the superior performance of CFQST columns, which consistently demonstrated the highest lateral load-carrying capacity, ductility, and energy dissipation capabilities among all column types. Key observations derived from this study are summarized as follows:

1. Superior lateral performance of CFQST columns: CFQST columns exhibited the highest lateral load-carrying capacity across all tested configurations, outperforming RCC, CFST, and CFDST columns. On average, CFQST columns showed a 133% increase in lateral capacity compared to RCC columns, 57% higher than CFST columns, and 20% higher than CFDST columns.

2. Enhanced ductility and energy dissipation: CFQST columns demonstrated significantly better ductility and energy dissipation capabilities, making them particularly suitable for seismic applications. The superior confinement provided by the external steel tube and internal steel elements contributed to their enhanced deformation capacities.
3. Influence of material properties and slenderness ratio: Increasing concrete strength improved the ultimate lateral load-carrying capacity but resulted in reduced ductility for all column types. Higher slenderness ratios were associated with reduced peak strength and increased displacement at failure.
4. Observed buckling modes: Elephant-foot buckling was the predominant failure mode in CFQST columns, highlighting the effectiveness of their design in delaying failure and maintaining stability under lateral loads.

These findings establish CFQST columns as a promising structural solution for high-performance applications, particularly in seismic-prone areas. Future work may be carried out to explore their long-term durability under cyclic loading, thermal effects, and other dynamic conditions, further validating their potential for widespread implementation

References

[1] Y. Dai, S. Nie, T. Zhou, C. Xue, and J. Peng, "Seismic Behavior Experimental Study on the Joint of Circular Tubed Steel-Reinforced Concrete Columns," *Shock and Vibration*, vol. 2021, no. 1, 2021.

[2] R. Jamalpour and K. M. A. Hossain, "Torsion and Combined Torsion-Axial Load Behaviour of Concrete Filled Steel Tube Columns with and without ECC/CFRP Wrap," *Journal of Earthquake Engineering*, vol. 28, no. 13, pp. 3744–3773, 2024.

[3] I. Azim, J. Yang, S. Bhatta, F. Wang, and Q. Liu, "Factors influencing the progressive collapse resistance of RC frame structures," *Journal of Building Engineering*, vol. 27, p. 100986, 2020.

[4] R. Couto, I. Sousa, R. Bento, and J. M. Castro, "Seismic vulnerability assessment of RC structures: research and practice at building level," *Elsevier eBooks*, pp. 31–84, 2022.

[5] A. Liaqat, H. F. Isleem, A. Bahrami, I. Jha, G. Zou, R. Kumar, A. M. Sadeq, and A. Jahami, "Integrated Behavioural Analysis of FRP-Confined Circular Columns using FEM and Machine Learning," *Composites Part C: Open Access*, pp. 100444–100444, 2024.

[6] I. Azim, J. Yang, S. Bhatta, F. Wang, and Q. Liu, "Factors influencing the progressive collapse resistance of RC frame structures," *Journal of Building Engineering*, vol. 27, p. 100986, 2020.

[7] S. Khusru, D. P. Thambiratnam, M. Elchalakani, and S. Fawzia, "Behaviour of Slender Hybrid Rubberised Concrete Double Skin Tubular Columns under Eccentric Loading," *Buildings*, vol. 14, no. 1, pp. 57–57, 2023.

[8] T. Qiong, I. Jha, A. Bahrami, H. F. Isleem, R. Kumar, and P. Samui, "Proposed numerical and machine learning models for fiber-reinforced polymer concrete-steel hollow and solid elliptical columns," *Frontiers of Structural and Civil Engineering*, vol. 18, no. 8, pp. 1169–1194, 2024.

[9] A. U. Amika, T. N. Haas, and L. Simwanda, "Multilinear regression model for predicting the ultimate load of slender circular CFDST columns subjected to concentric and eccentric loading," *Structural Concrete*, vol. 26, no. 3, pp. 3527-3545, 2024.

[10] I. Jha, and K. K. Pathak, "Synergetic concrete shape and cable layout optimization of pre-stressed concrete beams," *Structural and Multidisciplinary Optimization*, vol. 66, no. 87, 2023.

[11] I. Jha, K. K. Pathak, M. Jha, and A. Ranjan, "A comparative study of gradient descent method and a novel non-gradient method for structural shape optimization," *International Journal of Mathematical, Engineering and Management Sciences*, vol. 7, no. 2, pp. 258-271, 2022.

[12] Z. Tao, Z.-B. Wang, and Q. Yu, "Finite element modelling of concrete-filled steel stub columns under axial compression," *Journal of Constructional Steel Research*, vol. 89, pp. 121–131, 2013.